3-1-1990

Effects of bandwidth-limiting tuning elements in synchronously pumped mode-locked lasers

Bahram Zandi

Lee W. Casperson
Portland State University

Duncan Leo MacFarlane

Citation Details

Zandi, B., Casperson, L. W., & MacFarlane, D. L. (1990). Effects of bandwidth-limiting tuning elements in synchronously pumped mode-locked lasers. Journal Of Applied Physics, 67(5), 2229.

Effects of bandwidth-limiting tuning elements in synchronously pumped mode-locked lasers

Bahram Zandi,[a] Lee W. Casperson, and D. L. MacFarlane[b]
Department of Electrical Engineering, Portland State University, Portland, Oregon 97207

(Received 7 August 1989; accepted for publication 6 November 1989)

A description of bandwidth-limiting tuning filters is introduced into a semiclassical model for synchronously pumped mode-locked dye lasers. The finite phase memory of the molecular wave functions is included as are the isotropic molecular distribution and the finite vibrational relaxation times. The new set of equations has been solved numerically using the best available values for the various parameters. The results have been compared with experimental data obtained using a rhodamine 6G dye laser, which is synchronously pumped using an acousto-optically mode-locked argon laser. Tuning element effects have been studied using two- and three-plate birefringent filters and a tuning wedge, and the experimental results agree with the numerical solutions.

I. INTRODUCTION

Synchronous optical pumping is one of the most popular methods of producing tunable ultrashort pulses, and such pulses are finding an ever-increasing number of practical applications. Most previous studies of synchronously pumped mode-locked laser systems have used rate-equation analyses, which describe the laser dynamics in terms of the molecular population densities and photon densities.[1–16] A semiclassical model introduced previously has been the starting point for the present study.[17] The advantage of a semiclassical model in comparison to a rate-equation model is that a semiclassical model allows a rigorous treatment of the coherence effects resulting from the finite phase memory of the molecular wave functions. These coherence effects become especially important for small values of the length mismatch between the pump laser and the dye laser. The model adopted here also includes a vector description of the fields and molecular dipoles and a finite vibrational relaxation time of the lower state of the dye-laser transition.

The purpose of this study has been to enhance the semiclassical model described above so that it can rigorously describe the effects of commonly employed bandwidth-limiting tuning filters. The filter description is developed by analogy with the bandpass characteristics of nonsaturating two-level absorbers. The derivation of our model for a synchronously pumped mode-locked dye laser with a bandwidth-limiting tuning element is contained in Sec. II. Section III describes the extraction of the various model parameters from measurements on the laser components, and in Sec. IV the model is reduced to a compact normalized form. The values of the experimental parameters of our rhodamine 6G system are summarized in Sec. V, and a comparison of experimental results and theoretical predictions is included in Sec. VI.

II. THEORY

The energy-level model used in the treatment of the dye-laser amplifier is shown schematically in Fig. 1. The dye molecules in this model are assumed initially to be representable by a four-level system in which the pump absorption takes place between levels 0 and 3, while the signal-stimulated emission takes place between levels 2 and 1. The molecules in level 3 decay nonradiatively to level 2 with a vibrational relaxation time τ_3, while molecules in level 1 have a vibrational relaxation time of τ_1. The spontaneous decay time for the laser transition is represented by τ_2. The actual energy-level structure of the dye molecules is, of course, more complicated than this simple model would indicate, but the model is found to include the terms most important for synchronously pumped mode-locked dye lasers.

The procedure for setting up the semiclassical equations is well known, and for present purposes we take as our starting point Eqs. (24), (37), (38), and (40) of Ref. 17:

$$\frac{\partial \rho_{22}}{\partial t} = \frac{1}{\hbar}\,\mathrm{Im}(\eta_s \cdot \mathscr{E}_s^*) - \frac{\rho_{22}}{\tau_2} + \frac{T_p}{2\hbar^2}\,|\mu_p|^2\,|\mathscr{E}_p \cdot \hat{\mathbf{e}}_p|^2, \tag{1}$$

$$\frac{\partial \rho_{11}}{\partial t} = -\frac{1}{\hbar}\,\mathrm{Im}(\eta_s \cdot \mathscr{E}_s^*) - \frac{\rho_{11}}{\tau_1} + \frac{\rho_{22}}{\tau_2}, \tag{2}$$

$$\frac{\partial \eta_s}{\partial t} = i(\omega_s - \omega_{s0})\eta_s - \frac{i}{2\hbar}\,(\rho_{22} - \rho_{11})\,|\mu_s|^2 \mathscr{E}_s \cdot \hat{\mathbf{e}}_s - \frac{\eta_s}{T_s}, \tag{3}$$

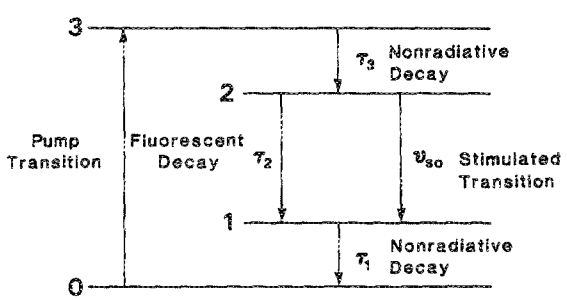

FIG. 1. Energy-level model used in the dye-laser analysis.

[a] Present address: Physical Sciences Laboratory, New Mexico State University, Las Cruces, New Mexico 88003.
[b] Present address: School of Engineering and Computer Science, The University of Texas at Dallas, Richardson, Texas 75083.

 0021-8979/90/052229-06$03.00

$$\frac{\partial \mathscr{E}_s}{\partial z}+\frac{1}{v}\frac{\partial \mathscr{E}_s}{\partial t}+\frac{\alpha_s}{2}\mathscr{E}_s=i\mu\frac{\omega_s^2}{k_s}\int_\Omega n(\theta,\phi)\eta_s\hat{\mathbf{e}}_s d\Omega, \quad (4)$$

where $\eta_s=\eta_s\hat{\mathbf{e}}_s$ is the complex polarization amplitude of the signal dipoles, $\mathscr{E}_p$ and $\mathscr{E}_s$ are the complex amplitudes of the pump and signal fields, ω_s is the signal frequency, ω_{s0} is the center frequency of the signal transition, μ_p and μ_s are the matrix elements of the pump and signal dipole moment operators, T_p and T_s are the coherence times of the off-diagonal density matrix elements, k_s and α_s are propagation and distributed loss coefficients, and $n(\theta,\phi)d\Omega$ is the number of molecules per unit volume oriented within the solid angle $d\Omega$ about the (θ,ϕ) direction.

Equations (1)–(4) provide a reasonably rigorous description of the fast dynamics of a dye-laser amplifier, and this model has been shown to provide good agreement with many of the observed features of a synchronously pumped mode-locked dye laser.[18–21] The next step in this analysis is to incorporate into the laser amplifier model a mathematical representation of a bandwidth-limiting tuning filter. The easiest way to obtain this representation is to recognize that the essential feaures of a typical bandwidth filter can be considered to be a special case of Eqs. (1)–(4). If one neglects pumping ($\mathscr{E}_p=0$) and lower state decay ($\tau_1=0$) and assumes a unidirectional molecular distribution [$n(\theta,\phi)=N_f\delta(\theta-\theta_0,\phi-\phi_0)$], Eqs. (1)–(4) reduce to

$$\frac{\partial \rho_f}{\partial t}=\frac{1}{\hbar}\,\mathrm{Im}(\eta_f\mathscr{E}_s^*)-\frac{\rho_f}{\tau_f}, \quad (5)$$

$$\frac{\partial \eta_f}{\partial t}=i(\omega_s-\omega_{f_0})\eta_f-\frac{i}{2\hbar}(2\rho_f-1)|\mu_f|^2\mathscr{E}_s\hat{\mathbf{e}}_f-\frac{\eta_f}{T_f}, \quad (6)$$

$$\frac{\partial \mathscr{E}_s}{\partial z}+\frac{1}{v}\frac{\partial \mathscr{E}_s}{\partial t}=i\mu\frac{\omega_s^2}{k_s}N_f\eta_f\hat{\mathbf{e}}_f-\frac{\alpha_f}{2}\mathscr{E}_s, \quad (7)$$

where N_f is the number of filter dye molecules per unit volume, the density matrix for the filter molecules is normalized as $\rho_f=\rho_{22f}=1-\rho_{11f}$, and the subscript f always refers to the filter.

If the absorbing filter dipoles are parallel to the electric field, Eqs. (5)–(7) reduce further to

$$\frac{\partial \rho_f}{\partial t}=\frac{1}{\hbar}\,\mathrm{Im}(\eta_f\mathscr{E}_s^*)-\frac{\rho_f}{\tau_f}, \quad (8)$$

$$\frac{\partial \eta_f}{\partial t}=i(\omega_s-\omega_{f0})\eta_f-\frac{i}{2\hbar}(2\rho_f-1)|\mu_f|^2\mathscr{E}_s-\frac{\eta_f}{T_f}, \quad (9)$$

$$\frac{\partial \mathscr{E}_s}{\partial z}+\frac{1}{v}\frac{\partial \mathscr{E}_s}{\partial t}=i\mu\frac{\omega_s^2}{k_s}N_f\eta_f-\frac{\alpha_f}{2}\mathscr{E}_s, \quad (10)$$

where $\mathscr{E}_s$ is the complex amplitude of the vector electric field $\mathscr{E}_s$. Equations (8)–(10) now represent a saturating filter. Most practical filter elements do not saturate, and to recognize that fact we may consider the limit $\tau_f\to 0$. In this limit $\rho_f=0$ and Eq. (9) can be written

$$\frac{\partial \eta_f}{\partial t}=i(\omega_s-\omega_{f0})\eta_f-\frac{i}{2\hbar}|\mu_f|^2\mathscr{E}_s-\frac{\eta_f}{T_f}. \quad (11)$$

Bandwidth-limiting filters are usually characterized in terms of their response to a steady-state monochromatic signal rather than their response to transient signals. In steady state Eq. (11) has the solution

$$\eta_f=\frac{iT_f|\mu_f|^2\mathscr{E}_s/2\hbar}{1-i(\omega_s-\omega_{f0})T_f}. \quad (12)$$

To the extent that this familiar Lorentzian function can represent the steady-state bandpass characteristics of a tuning filter, equations like Eqs. (10) and (11) can be used to describe the transient response.

For simplicity we will only consider the case in which the laser signal and the bandpass filter are tuned to the center frequency of the laser transition ($\omega_s=\omega_{s0}=\omega_{f0}$). The filter bandpass is generally narrow compared to the gain bandwidth, and with the normalization described below, detuning from the center of the laser transition is expected to have little effect. With this restriction the complex electric field amplitude $\mathscr{E}_s$ can be considered to be purely real while the polarization amplitudes η_s and η_f may be replaced by the imaginary terms $i\eta_s'$ and $i\eta_f'$. With these reductions Eqs. (1)–(4), (10), and (11) can be combined together into the set

$$\frac{\partial \rho_{22}}{\partial t}=\frac{1}{\hbar}\eta_s\mathscr{E}_s x-\frac{\rho_{22}}{\tau_2}+\frac{T_p}{2\hbar^2}|\mu_p|^2\mathscr{E}_p^2x^2, \quad (13)$$

$$\frac{\partial \rho_{11}}{\partial t}=-\frac{1}{\hbar}\eta_s\mathscr{E}_s x-\frac{\rho_{11}}{\tau_1}+\frac{\rho_{22}}{\tau_2}, \quad (14)$$

$$\frac{\partial \eta_s'}{\partial t}=-\frac{1}{2\hbar}(\rho_{22}-\rho_{11})|\mu_s|^2\mathscr{E}_s x-\frac{\eta_s'}{T_s}, \quad (15)$$

$$\frac{\partial \eta_f'}{\partial t}=\frac{1}{2\hbar}|\mu_f|^2\mathscr{E}_s-\frac{\eta_f'}{T_f}, \quad (16)$$

$$\frac{\partial \mathscr{E}_s}{\partial z}+\frac{1}{v}\frac{\partial \mathscr{E}_s}{\partial t}=-\mu\frac{\omega_s^2}{k_s}N_s\int_0^1\eta_s' x\,dx+\mu\frac{\omega_s^2}{k_s}N_f\eta_f'-\frac{\alpha_s}{2}\mathscr{E}_s-\frac{\alpha_f}{2}\mathscr{E}_s-\frac{\alpha_m}{2}\mathscr{E}_s, \quad (17)$$

where the orientational distribution of the dye molecules in the laser amplifier has been assumed to be isotropic according to $n(\theta,\phi)=N_s/4\pi$. The absorption and emission dipoles are assumed to be parallel ($\hat{\mathbf{e}}_p=\hat{\mathbf{e}}_s$), the pump and signal field polarizations are assumed to be parallel to the x axis, and $\mathscr{E}_p$ is taken to be real. The new variable $x=\cos\theta$ measures the angle between the fields and the laser dipoles. The sign of the filter interaction term in the field equation has been reversed to acknowledge that we want the filter to be a bandpass device rather than the notch filter that follows from our nonsaturating two-level absorber model. The term α_f indicates that outside the Lorentzian bandpass of the tuning filter there is still a residual loss, and α_m is a distributed representation of the mirror losses.

III. PARAMETER EVALUATION

Before Eqs. (13)–(17) can be integrated, it is necessary to have explicit values for all of the parameters involved. The essence of this evaluation is the assumption that all elements

of the laser system (amplifier, filter, and mirrors) may be assumed to be distributed uniformly over the length l_a of the laser amplifier. If $T_{\min}$ represents the single-pass residual intensity transmission away from the filter bandpass region, then the corresponding effective distributed loss coefficient α_f must be related to the input and output intensities by

$$I_2 = T_{\min} I_1 = I_1 \exp(-\alpha_f l_a). \tag{18}$$

Therefore the filter loss coefficient is given explicitly by

$$\alpha_f = -\frac{\ln(T_{\min})}{l_a}. \tag{19}$$

Similarly, the mirror reflectivities may be associated with a double pass through the laser amplifier using the relationship

$$I_2 = R_1 R_2 I_1 = I_1 \exp(-2\alpha_m l_a). \tag{20}$$

Therefore the mirror loss coefficient is given explicitly by

$$\alpha_m = -\frac{\ln(R_1 R_2)}{2l_a}. \tag{21}$$

These losses may be combined into a single total loss coefficient α given by

$$\alpha = \alpha_s + \alpha_f + \alpha_m = \alpha_s - \frac{\ln(T_{\min})}{l_a} - \frac{\ln(R_1 R_2)}{2l_a}. \tag{22}$$

It will also be necessary to establish the effective line-center cw gain coefficient of the tuning filter, which is now considered to be a narrow-band nonsaturating amplifier. This gain g_f can be obtained from the actual filter parameters by means of the relationship

$$I_2 = \frac{T_{\max}}{T_{\min}} I_1 = I_1 \exp(g_f l_a), \tag{23}$$

where $T_{\max}$ is the maximum transmission of the bandpass-limiting filter. Therefore the filter gain coefficient is given by

$$g_f = [\ln(T_{\max}/T_{\min})]/l_a. \tag{24}$$

The final coefficient to be derived is the effective coherence time T_f of the bandpass filter in terms of other measurable quantities. First, it may be seen from Eq. (12) that the full width at half maximum of a homogeneously broadened absorber is related to the coherence time by

$$T_f = (\pi \Delta\nu_h)^{-1}. \tag{25}$$

On the other hand, the measured bandwidth of a distributed amplifier (or tuning filter) of length l_a is related to the homogeneous linewidth by the formula[22]

$$\Delta\nu_f = \Delta\nu_h \left(\frac{g_f l_a}{\ln[\exp(g_f l_a) + 1] - \ln 2} - 1 \right)^{1/2}. \tag{26}$$

Combining Eqs. (25) and (26) one finds that the filter coherence time can be related to the filter gain coefficient by

$$T_f = \frac{1}{\pi \Delta\nu_f} \left(\frac{g_f l_a}{\ln[\exp(g_f l_a) + 1] - \ln 2} - 1 \right)^{1/2}, \tag{27}$$

and thus all of the new elements of the distributed filter model have been expressed in terms of easily measurable characteristics of a practical tuning filter.

IV. NORMALIZATION

As a next step, Eqs. (13)–(17) can be written in a more compact form if one introduces normalized expressions for the dependent variables. To the extent possible we employ the same notation used previously,[17] and thus we adopt the forms

$$D = \frac{\mu \omega_s^2 N_s T_s |\mu_s|^2}{k_s \hbar \alpha} (\rho_{22} - \rho_{11}), \tag{28}$$

$$M = \frac{\mu \omega_s^2 N_s T_s |\mu_s|^2}{k_s \hbar \alpha} (\rho_{22} + \rho_{11}), \tag{29}$$

$$Q = -\frac{\mu \omega_s^2 N_s |\mu_s| (2\tau_2 T_s)^{1/2}}{k_s \hbar \alpha} \eta_s', \tag{30}$$

$$F = \frac{|\mu_s| (2\tau_2 T_s)^{1/2}}{|\mu_f|^2 T_f} \eta_f', \tag{31}$$

$$A = \frac{|\mu_s|}{\hbar} \left(\frac{\tau_2 T_s}{2} \right)^{1/2} \mathscr{E}_s, \tag{32}$$

$$P = \frac{\mu \omega_s^2 N_s T_s |\mu_s|^2}{k_s \hbar \alpha} \frac{\tau_2 T_p |\mu_p|^2 \mathscr{E}_p^2}{2\hbar^2}. \tag{33}$$

Here D is a normalized population difference, M is a normalized population sum, Q is a normalized amplifier polarization, F is a normalized filter polarization, A is a normalized field, and P is a normalized pump rate. In terms of these new variables, Eqs. (13)–(17) can be written

$$\frac{\partial D}{\partial t} = -\frac{1}{\tau_2} \left[\left(1 + \frac{\tau_2}{2\tau_1} \right) D + \left(1 - \frac{\tau_2}{2\tau_1} \right) M + 2QAx - Px^2 \right], \tag{34}$$

$$\frac{\partial M}{\partial t} = -\frac{1}{\tau_2} \left(-\frac{\tau_2}{2\tau_1} D + \frac{\tau_2}{2\tau_1} M - Px^2 \right), \tag{35}$$

$$\frac{\partial Q}{\partial t} = -\frac{1}{T_s} (Q - ADx), \tag{36}$$

$$\frac{\partial F}{\partial t} = -\frac{1}{T_f} (F - A), \tag{37}$$

$$\frac{\partial A}{\partial z} + \frac{1}{v} \frac{\partial A}{\partial t} = -\frac{\alpha}{2} \left(A - \int_0^1 Qx\, dx - \frac{g_f}{\alpha} F \right), \tag{38}$$

where again g_f is the effective cw gain coefficient of the tuning filter for a cw signal [$F = A$ from Eq. (37)].

Equations (34)–(38) now form a complete set describing the evolution of a short pulse of light in a medium having various distributed gain and loss characteristics. These equations may be readily applied to the problem of periodic pulse circulation in a laser oscillator. This is accomplished by introducing a new time coordinate $\tau = t - z/v_s$, where v_s is the speed in the laser of all quantities of interest. Then Eqs. (34)–(38) reduce to the ordinary differential equations

$$\frac{dD}{d\tau} = -\frac{1}{\tau_2} \left[\left(1 + \frac{\tau_2}{2\tau_1} \right) D + \left(1 - \frac{\tau_2}{2\tau_1} \right) M + 2QAx - Px^2 \right], \tag{39}$$

$$\frac{dM}{d\tau} = -\frac{1}{\tau_2}\left(-\frac{\tau_2}{2\tau_1}D + \frac{\tau_2}{2\tau_1}M - Px^2\right), \tag{40}$$

$$\frac{dQ}{d\tau} = -\frac{1}{T_s}(Q - ADx), \tag{41}$$

$$\frac{dF}{d\tau} = -\frac{1}{T_f}(F - A), \tag{42}$$

$$\frac{dA}{d\tau} = -\frac{\alpha v}{2(1 - v/v_s)}\left(A - \int_0^1 Qx\,dx - \frac{g_f}{\alpha}F\right). \tag{43}$$

The pulse speed in the laser v_s can also be related to the cavity length L and the round-trip time t_{RT} (or mode-locking period), and a more useful alternate formulation of Eq. (43) is[17]

$$\frac{dA}{d\tau} = -\frac{L}{2t_c\Delta L}\left(A - \int_0^1 Qx\,dx - \frac{g_f}{\alpha}F\right), \tag{44}$$

where the intensity loss coefficient has been replaced by the usual photon cavity lifetime $t_c = L/\alpha v l_a$.

It is also necessary to specify the pump function $P(\tau)$. In our modeling, we have used the function $P(\tau) = P_0 f(\tau)$, where $f(\tau)$ is the normalized function

$$f(\tau) = \frac{2}{\Delta\tau}\left(\frac{\ln 2}{\pi}\right)^{1/2}\exp\left[-\left(\frac{2\tau}{\Delta\tau}\right)^2 \ln 2\right], \tag{45}$$

with $\Delta\tau$ being the full width at half maximum. It is helpful to relate the pump amplitude to a threshold parameter r, which measures the ratio of the actual pump amplitude P_0 to the amplitude that would just bring the gain value up to the loss value by the end of the pump pulse. From Eq. (44) this threshold parameter would be given by the maximum value of the ratio

$$\frac{\int_0^1 Qx\,dx}{(1 - g_f/\alpha)A},$$

and from Eqs. (39), (41), and (45) the value of Q can be approximated by

$$Q = ADx = \frac{AP_0x^3}{\tau_2}. \tag{46}$$

Thus the threshold parameter is related approximately to P_0 by

$$r = \frac{P_0}{5\tau_2(1 - g_f/\alpha)}. \tag{47}$$

V. DATA

It is now necessary to specify the various fundamental parameter values used in our experiments. Many of these values are simply adopted from Ref. 17 and include the fluorescence decay time $\tau_2 = 5\times10^{-9}$ s, the vibrational relaxation time $\tau_1 = 1\times10^{-12}$ s, the coherence time $T_s = 5\times10^{-14}$ s, and the length $L = 1.8$ m. The mirror reflectivities are $R_1 \approx 1$ and $R_2 \approx 0.93$. The pump pulse width in our experiments is measured to be $\Delta\tau \approx 80$ ps, and the threshold parameter is adjusted to $r = 2$.

The parameters of the bandwidth-limiting tuning filters used in our studies have been determined experimentally. The specific filters employed include a tuning wedge and two birefringent filters. For the characterization of the tuning wedge a Cary 14 spectrophotometer was used, and for the birefringent filters the dye laser was used in combination with a Jarrell-Ash Monospec/50 monochromator. The resulting transmission curves for these filters are shown in Figs. 2(a)–2(c), and the inferred parameter values are summarized in Table I, assuming the transmission maximum is at about $\lambda = 600$ nm. The values listed in the table are used in our computer model to determine the various parameters discussed in Sec. III above.

VI. RESULTS

A series of experiments has been carried out to verify the theoretical model. In these experiments an acousto-optically mode-locked argon-ion laser (Spectra-Physics Model 2020-05) was used to synchronously pump a rhodamine 6G dye

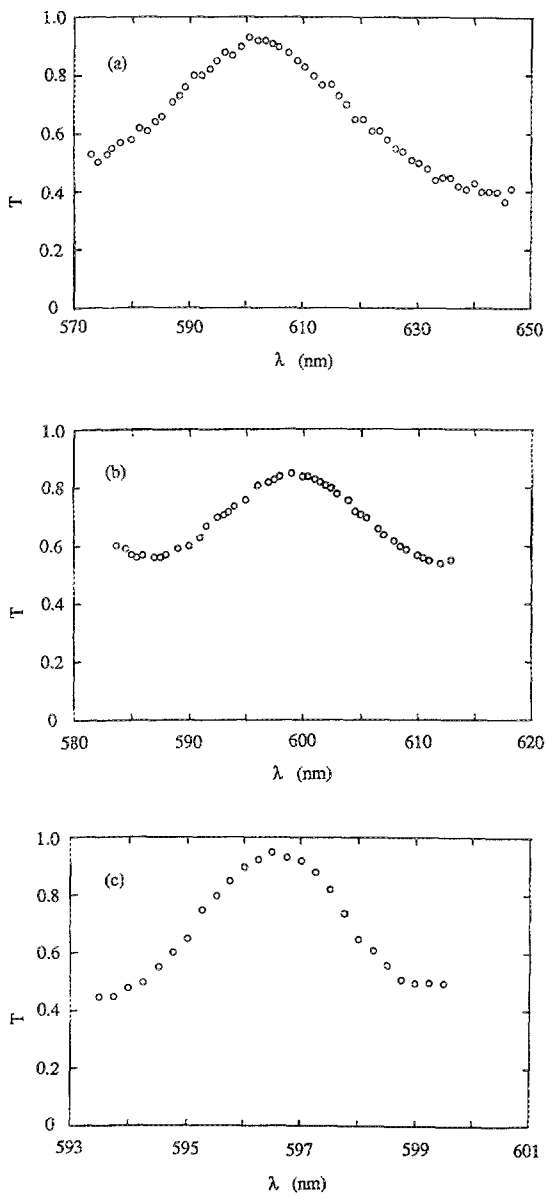

FIG. 2. Transmission functions for (a) tuning wedge filter, (b) two-plate birefringent filter, and (c) three-plate birefringent filter.

TABLE I. Tuning filter properties.

	Tuning wedge	Two-plate birefringent	Three-plate birefringent
T_{max}	0.93	0.85	0.94
T_{min}	0.40	0.55	0.47
$\Delta\lambda$ (nm)	34	13	2.7
$\Delta\nu$ (Hz)	28×10^{12}	11×10^{12}	2.3×10^{12}

laser (Spectra Physics Model 375B). The argon laser is mode locked using an acousto-optic prism that also forces the laser to operate only on the 514.5-nm line. The lasing medium in the dye laser consists of rhodamine 6G in ethylene glycol. The output coupler of the dye laser is mounted on a precision translatable stage, which provides the cavity length adjustment. A Mitutoyo dial indicator permits relative displacement measurements readable to 0.5-μm resolution. As noted previously, bandwidth effects have been studied using two- and three-plate birefringent filters and a tuning wedge. The essence of our experimental study has been to compare the autocorrelated dye-laser pulses with the predictions of the theoretical model. The autocorrelated pulses have been measured as a function of the length detuning using a Spectra-Physics Model 409 Scanning Autocorrelator. The theoretical autocorrelations were obtained using the formula

$$G^2(\tau') = \int_{-\infty}^{\infty} I(\tau)I(\tau+\tau')d\tau, \tag{48}$$

where the intensity $I = A^2$ is the square of the field amplitude A governed by Eq. (44).

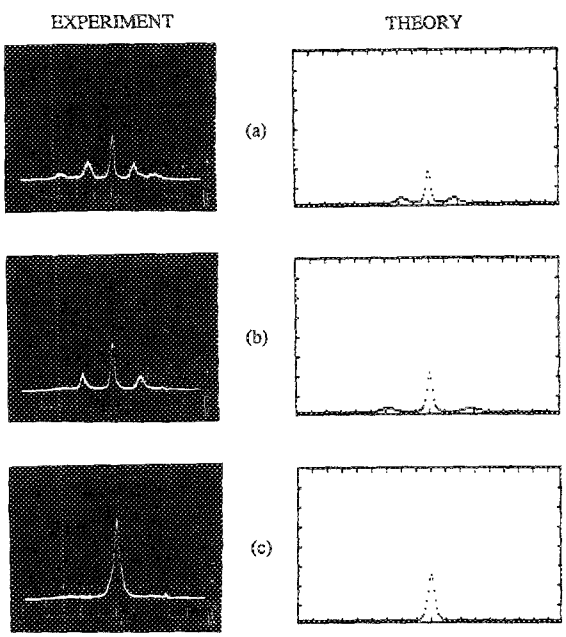

FIG. 3. Experimental and theoretical autocorrelations for a synchronously pumped mode-locked rhodamine 6G laser with a two-plate birefringent filter and length detunings of (a) 3 μm, (b) 6 μm, and (c) 11 μm. In the experimental waveforms the time scale is 5 ps per division and in the theoretical waveforms the time scale is 3 ps per division.

A typical comparison between the experimental and theoretical autocorrelations is shown in Fig. 3 for a laser containing the two-plate birefringent filter. The absolute length detunings are obtained from the relative detunings by best-fitting a large set of experimental and theoretical detuning autocorrelations for each bandpass filter. Good agreement is obtained concerning both the pulse widths and the pulsation echoes that occur for small positive length detunings of the dye laser. A large amount of data like those shown in Fig. 3 can be summarized by plotting autocorrelation pulse widths versus length detunings. A series of these plots

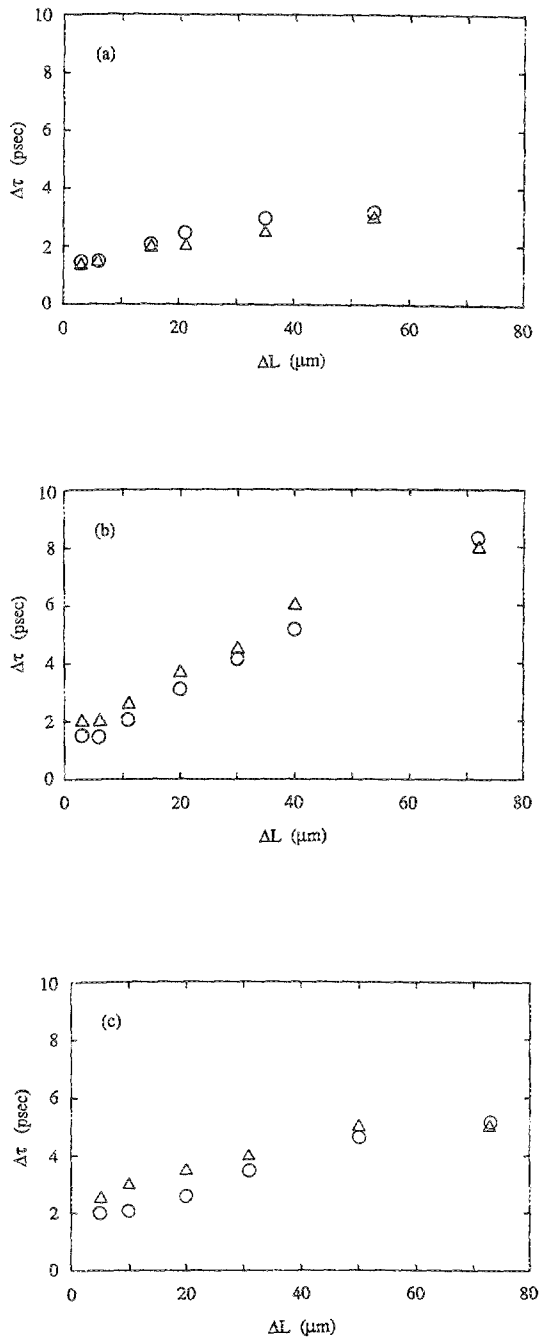

FIG. 4. Experimental (○) and theoretical (△) autocorrelation widths as functions of length detuning for (a) tuning wedge filter, (b) two-plate birefringent filter, and (c) three-plate birefringent filter.

is included in Fig. 4 for the tuning wedge, the two-plate filter, and the three-plate filter with all other laser parameters kept constant. Agreement is obtained between theory and experiment under a wide range of conditions. The discrepancies are not much larger than the uncertainty in determining the pulse widths and may be due to errors in estimating some of the laser parameter values and to simplifications made in deriving the model. The shortest pulses are obtained with small length detunings and use of the broader tuning filters.

VII. CONCLUSION

A semiclassical model has been developed for describing synchronously pumped mode-locked dye lasers producing picosecond pulses. The model includes a rigorous description of the effects of a fairly general bandwidth-limiting tuning filter as well as a finite phase coherence time of the molecular wave functions, isotropic molecular distribution, and finite vibrational relaxation time. The new set of equations has been solved numerically using the best available values for the various parameters of a rhodamine 6G system, and autocorrelations have been computed for a range of length detunings and a variety of bandwidth-limiting elements. The experimental pulse shapes agree well with the theoretical solutions for all values of detuning and filter bandwidth. Thus the model should be useful for designing optimized synchronously pumped mode-locked laser systems.

ACKNOWLEDGMENTS

This work was supported in part by the National Science Foundation under Grant No. ECS-8511593 and by Tektronix, Inc.

[1]Z. A. Yasa and O. Teschke, Opt. Commun. **15**, 169 (1975).
[2]A. Scavennec, Opt. Commun. **17**, 14 (1978).
[3]Z. A. Yasa, Appl. Phys. B **30**, 135 (1983).
[4]G. H. C. New and J. M. Catherall, Opt. Commun. **50**, 111 (1984).
[5]W. Heudorfer and G. Marowsky, Appl. Phys. **17**, 181 (1978).
[6]P. G. Kryukov and V. S. Letokhov, Sov. Phys. Usp. **12**, 641 (1970).
[7]D. Faubert and S. L. Chin, Can. J. Phys. **57**, 1359 (1979).
[8]D. M. Kim, J. Kuhl, R. Lambrich, and D. von der Linde, Opt. Commun. **27**, 123 (1978).
[9]A. E. Siegman and D. J. Kuizenga, Opto-Electron. **6**, 43 (1974).
[10]C. P. Ausshnitt and R. K. Jain, Appl. Phys. Lett. **32**, 727 (1978).
[11]C. P. Ausshnitt, R. K. Jain, and J. P. Heritage, IEEE J. Quantum Electron. **QE-15**, 912 (1979).
[12]J. Herrmann and U. Motschmann, Opt. Commun. **40**, 379 (1982).
[13]J. Herrmann and U. Motschmann, Appl. Phys. B **27**, 27 (1982).
[14]L. M. Davis, J. D. Harvey, and J. M. Peart, Opt. Commun. **50**, 49 (1984).
[15]T. Urisu and Y. Mizushima, J. Appl. Phys. **57**, 1518 (1985).
[16]J. M. Catheral, G. H. C. New, and P. M. Radmore, Opt. Lett. **7**, 319 (1982).
[17]L. W. Casperson, J. Appl. Phys. **54**, 2198 (1983).
[18]B. Zandi and L. W. Casperson, Opt. News **14**(9), 145 (1988).
[19]D. L. MacFarlane and L. W. Casperson, J. Opt. Soc. Am. B **6**, 292 (1989).
[20]D. L. MacFarlane and L. W. Casperson, Opt. Lett. **14**, 314 (1989).
[21]D. L. MacFarlane and L. W. Casperson, J. Opt. Soc. Am. B **6**, 1175 (1989).
[22]L. W. Casperson and A. Yariv, IEEE J. Quantum Electron. **QE-8**, 80 (1972).